MATEC Web of Conferences **72**, 01071 (2016) DOI: 10.1051/matecconf/20167201071
HMTTSC-2016

DYNAMICS OF EVAPORATION FRONT PROPAGATION IN FREON R21 WITH ADDITION OF NANOPARTICLES

Mikhail Moiseev[1,*], *Denis* Kuznetsov[1], and *Vladimir* Zhukov[1]

[1]Kutateladze Institute of Thermophysics SB RAS, Novosibirsk

Abstract. The paper presents the results of an experimental study on propagation dynamics of the self-sustained evaporation front in a large volume of Freon-R21 with the addition of SiO_2 nanoparticles. The experimental data on propagation velocity and structure of evaporation fronts were obtained; the spectral analysis of fluctuations of the evaporation front interface was carried out. The characteristic frequencies and amplitudes of interface fluctuations were determined depending on the velocity of evaporation front propagation. It was shown that the addition of nano-sized particles significantly affects the front velocity and character of interface fluctuations.

1 Introduction

The task of intensification of heat removal from the heated wall by means of phase transition has more than a century history. The steam boilers and reactors at nuclear power plants, heat pipes and film distillation apparatuses of cryogenic and chemical enterprises [1], spray heat exchanging systems [2], cooling systems for superconductors and processors of supercomputers: all of them use the heat of phase transition for heat transportation from the hot source. Usual water and organic, cryogenic liquids, and liquid mixtures and solutions are usually used as the working liquids [3, 4]. Limiting the intensity of heat removal is caused by formation of a vapor film near the heat transfer surface and, in particular, it is determined by the dynamics of this film propagation along the heating surface [5, 6].

In the last decade there has been a tendency to use nanofluids for heat transfer intensification both in the systems without phase transition, due to improvement of thermal physical properties of liquid [7], and in systems with phase transition, due to expansion of the area of nucleate boiling because of an increase in the value of the first critical heat flux in nanofluids [8]. Nanofluids may be a promising substitute for the classical liquids used as coolants in different applications. In most studies dealt with nanofluids, heat transfer is studied under the steady-state conditions. There are few studies of critical phenomena at non-stationary heat release in nanofluids. As an example, we can present [9], where the authors conducted the experiments on cooling the heated rods in nanofluid and observed a

* Corresponding author: moiseevmikhail@gmail.com

significant improvement in the cooling rate as compared to the pure liquid. The practical importance of these studies is caused by the necessity to develop the reliable protection systems for emergency decompression of devices containing nanofluids at high pressures and temperatures (e.g., future nuclear reactors, using nanofluids as a coolant).

The aim of this work is an experimental study of dynamics of propagation of the self-sustained evaporation front in nanofluids, including the study of the effect of nanoparticles on dynamic and structural characteristics of fluctuations of the evaporation front interface.

2 Research setup and experimental methods

Experiments were carried out in Freon R21 at reduced pressures P/P_c= 0.037 (0.193 MPa). For experimental studies of heat transfer and transient dynamics at non-stationary heat release under free convection the setup, shown schematically in fig. 1, was developed.

On bed 1, the frame 2 with refill tank 3 and working chamber 4, housing the working section 10, is hinged. The working chamber is a sealed cylindrical stainless steel vessel. The inner diameter of the chamber is 250 mm, and the height of the workspace is 250 mm. The working chamber is equipped with four windows 5. The bellows 6 with an adjusting screw 7 allows creating the required pressure (up to 0.4 MPa) in the working chamber at the closed valve 8. To set the desired temperature of liquid in the bottom of the chamber, heat exchanger 9 was located. Thus, using this working chamber, it is possible to perform experiments both with the fluid in equilibrium with vapor, and under the conditions of substantial subcooling (to saturation temperature). Frame hinging on the bed allows turning the chamber in relation to the vector of gravity.

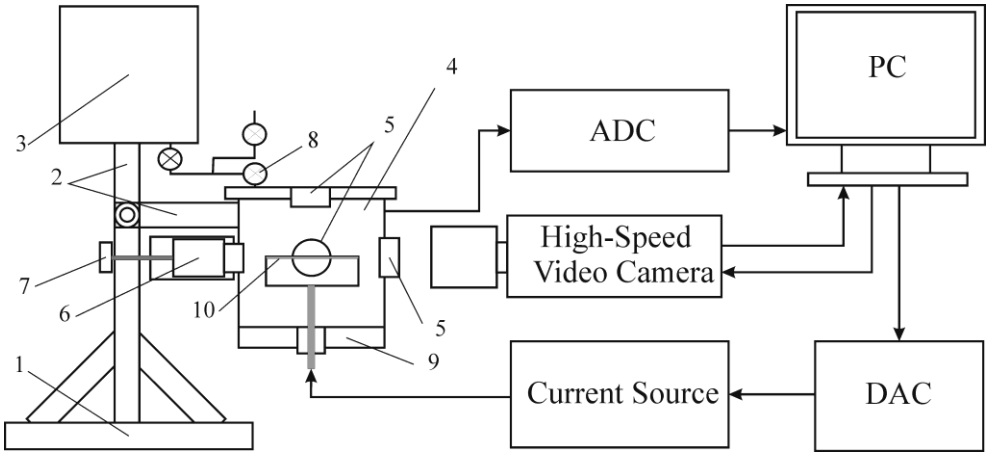

Fig. 1. Scheme of experimental setup.

The working section was made of the stainless steel tube. A thin-film platinum thermometer was installed inside the tube to measure the temperature in the quasi-stationary regimes. The tube ends were hermetically sealed. The tube was heated by electric current passing through the tube. Two conductors of 0.05-mm diameter were welded in the middle of the tube to measure the voltage drop in the region of 31-mm length. In the experiments, two tubular working sections of stainless steel were used. Sections *No. 1* and *No. 2* had outer diameter of 3 mm, wall of 0.5 mm and length of 50 mm. Surface roughness of section *No. 1* was presented by transverse marks with the width of 5-25 μm, and surface roughness of section *No. 2* was presented by large cavities with 100-150 μm radius and

depth of 20 μm. In addition, the surface of section *No. 2* had a granular structure with the grains of 5 - 20 μm.

The step-wise current pulse was supplied to the working section. Since inertia in the section was rather high, wall heating occurred at the times of the evaporation front development (about 50 ms) with almost a constant rate (the initial section of the exponent). The heating rate of the heat transfer surface was 4500 K/s. The heat-transfer surface was heated to the desired temperature by pulse time variation. Stepped current interruption stopped heat generation in the working area, and the wall temperature remained virtually constant at the times of the evaporation front propagation ($dT/dt = 0$ K/s). Numerical calculation using thermal conductivity equations has shown that for the time of front passage (much lesser than the time of convection development) the wall temperature before the front varied not more than by 0.2 K. Thus in each experiment, the propagation of self-sustained evaporation front was investigated at the pre-set constant wall temperature.

The working section temperature, average over the length, was measured using temperature dependence of the section resistance. For this purpose, in the middle part of each working section, the voltage drop was measured in the segment of 31 mm. In each measurement, calibration was performed by the temperature of undisturbed fluid. This technique allowed measuring the average temperature of the working section with an error less than 3 K.

Dynamics of the measured wall temperature change was compared with the calculation for non-stationary thermal conductivity regime. Comparison of temperature difference, measured in transient process, at the times lesser than the time of convection development, showed excellent agreement of the experiment and numerical calculation. Until the moment of liquid boiling up, time dependence of the instantaneous wall temperature was determined on the volt-ampere characteristic of the working section. Since the vapor phase formation on the measured part of the working section, the wall temperature was determined based by the equations of non-stationary thermal conductivity. This approach is valid at rather large rates of the working area heating, when the convective mechanism of heat removal from the wall has no time to develop.

Visual observations of the dynamics of vapor phase formation and propagation on the heat-releasing surface were registered by a high-speed digital video camera Phantom v7.0. The shooting rate was usually 25 000 frames per second with the exposure of 26 microseconds. To measure the velocity of vapor front propagation, the camera software was used. When analyzing the results of high-speed digital video-shooting, using specially developed software, the line of the interfacial boundary in the propagating front was determined on each frame. The obtained data served to determine the average velocity of the front V_{fr}. Measurement error of the average velocity in the section of 6-12 mm along the heater did not exceed 0.05 m/s.

The used additives were SiO_2 particles that had an average size of 20 nm and hydrophilic properties. The powder was loaded into the working volume, then vacuum exhaust, filling with freon and multiple mixing were performed. Particle concentration was 0.0077% vol.

3 Experimental results

Dependence of the average velocity of evaporation front V_{fr} on wall superheat is shown in fig. 2. As can be seen from the diagram, there are two areas with different rates of a change in the vapor front velocity, depending on the temperature rise. In the area of low overheating, the growth rate of the front velocity vs. wall superheat is satisfactorily described through the calculation by the model [5]. In the area of high overheating, the

significantly higher growth rate of the front velocity vs. wall overheating is observed. In [5] it was suggested that this effect relates to intensification of heat transfer across the interface due to development of Landau instability [10]. In pure liquid, the data for different heaters coincide within the error. In nanofluids on both heaters, front initiating takes place at substantially higher overheating than in the pure liquid (approximately 55 K and 34 K, respectively). In the overheating range of 55-65 K the front velocities in nanofluids are equal or less than those in a pure liquid, but when the higher temperature pressures are achieved, the front velocity in nanofluids increases significantly. This effect is more pronounced for the heater No.1 with a lesser degree of surface roughness. In successive series of experiments, the front velocity in nanofluids increased (fig. 3).

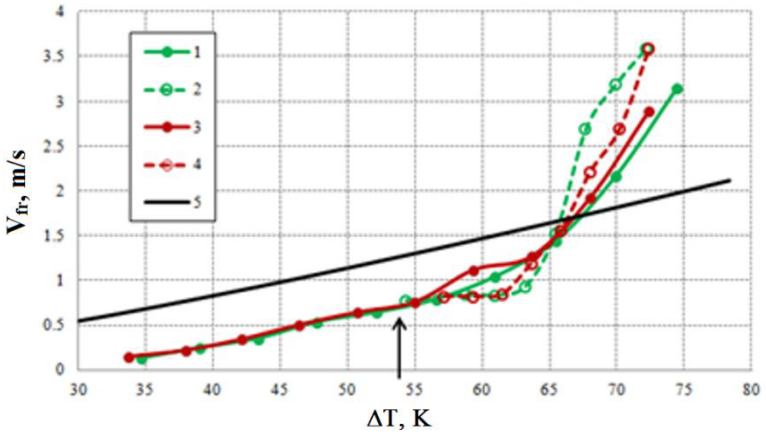

Fig. 2. Average front velocity vs. wall superheat. 1 – heater No.1, pure R21; 2 – heater No.1, R21 + 0.0077% SiO_2; 3 – heater No.2, pure R21; 4 – heater No. 2, R21 + 0.0077% SiO_2; 5 – calculation by model [5]. The arrow indicates the minimal value of overheating, when the evaporation front is initiated in nanofluid.

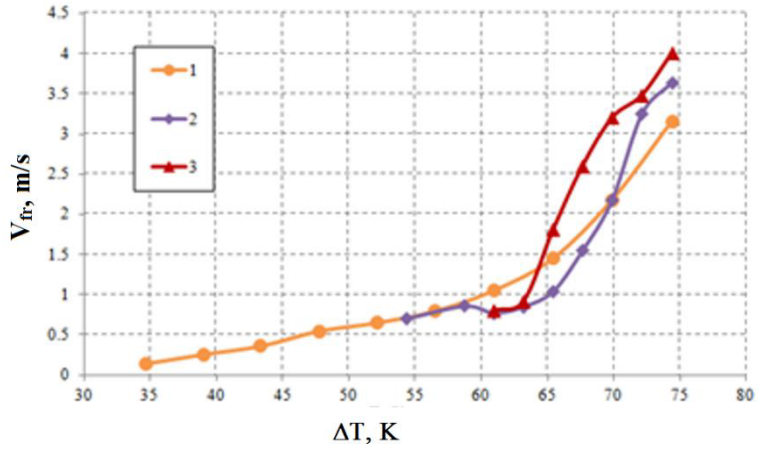

Fig. 3. Front velocity vs. wall superheat on heater No. 1 in different experimental series. 1 – pure R21; 2 – R21 + 0.0077% SiO_2 in two days nanoparticles addition; 3 - R21 + 0.0077% SiO_2 in nine days.

To investigate pulsations of the front interface, we used the dependence of x coordinate on time over one of the heater generatrices, i.e. for the fixed value of y-coordinate. The linear trend, complying with the distance run at constant speed V_{fr}, was deducted from the

resulting dependence. The fast Fourier transformation was applied to coordinate deviations from the path at a constant velocity. In all the spectra, the pronounced peak of main harmonic was observed. Using the amplitude and frequency of the main harmonic, we determined the characteristic velocity pulsations and acceleration of the interface.

Dependences of frequency and amplitude of the main harmonic on average velocity for heater No. 1 are shown in fig. 4. In pure liquid, the frequency of the main harmonic increases with a rise of the average velocity, and the amplitude decreases first and then achieves a constant value. The similar tendency is observed, but fluctuation frequencies and amplitudes decrease in comparison with pure liquid.

The amplitude value of interface acceleration, defined as the product of main harmonic amplitude on the square of angular frequency, can be estimated by data obtained. In pure liquid, acceleration varied within 50-1500 m/s^2 depending on wall overheating. In nanofluids, interface acceleration was several times lower than in the pure liquid, and it decreased in the successive series of experiments (fig. 5).

It is shown in [11] that interface acceleration affects significantly the instability development and intensification of heat transfer through the interface. A decrease in acceleration at nanoparticles addition gives an opportunity for instability development at the lower velocities of evaporation front.

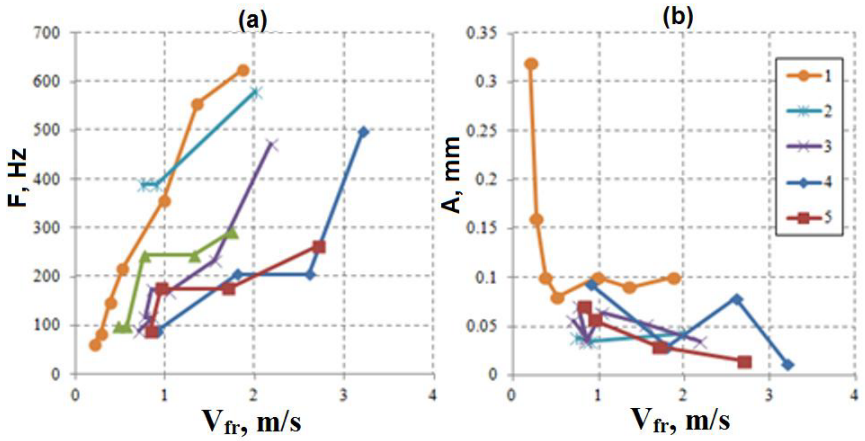

Fig. 4. (a) – frequencies and (b) – amplitudes of fluctuations of the front interface on heater No. 1 depending on average velocity. 1 – pure R21; 2 – R21 + 0.0077% SiO_2 in a day after nanoparticles addition; 3 – R21 + 0.0077% SiO_2 in two days; 4 - R21 + 0.0077% SiO_2 in nine days (series 1); R21 + 0.0077% SiO_2 in nine days (series 2).

The detected dependence of velocity and amplitude-frequency characteristics of fluctuations of evaporation front interface on the number of experimental series supports the effect of deposition of nanoparticles and their agglomerates on the heater wall at intense liquid evaporation at front propagation. However, a significant increase in the temperature difference, required for front initiation, was observed in the first experimental series with nanoparticles, and it is not explained by the effect of particles deposition.

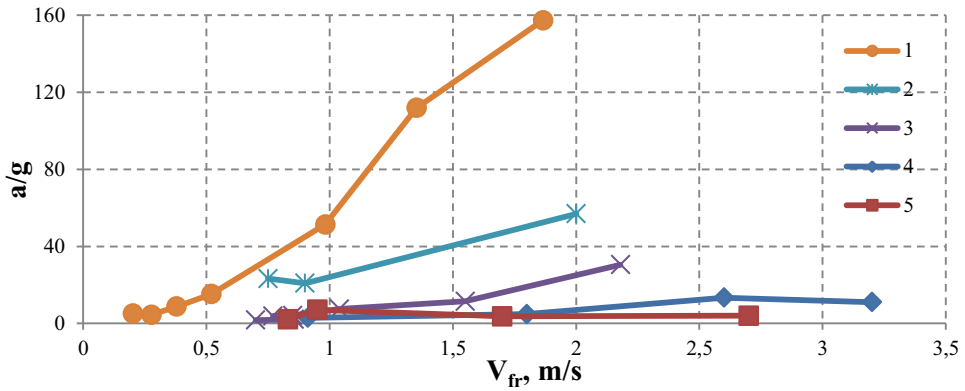

Fig. 5. Amplitude acceleration of the interf ace vs. average velocity. 1 – pure R21; 2 – R21 + 0.0077% SiO_2 in a day after nanoparticles addition; 3 – R21 + 0.0077% SiO_2 in two days; 4 - R21 + 0.0077% SiO2 in nine days (series 1); 5 - R21 + 0.0077% SiO_2 in nine days (series 2).

4 Conclusions

The evaporation front is initiated in the nanofluid at significantly higher wall overheating than in the pure liquid. Addition of nanoparticles into liquid significantly increases the velocity of evaporation front in the area of high overheating of the heating surface. Perhaps, this effect is associated with deposition of nanoparticles and their agglomerates on the heating surface. The effects caused by the addition of nanoparticles are more obvious for the heater with lower surface roughness. In pure liquid, we do not observe the effect of surface roughness on the characteristics of evaporation front. The effect of addition of nano-sized particles on the earlier development of instability has no an unambiguous explanation and requires following examination.

Acknowledgment

The work was financially supported by RFBR (project No. 13-08-00178-a).

References

1. A.N. Pavlenko, V.E. Zhukov, N.I. Pecherkin, V.Yu. Chekhovich, O.A. Volodin, A. Shilkin, and C. Grossmann, AIChE J **60(2)**, 690 (2014)
2. S.Y. Misyura, Int. J. Heat Mass Transfer **71**, 197 (2014)
3. V.E. Nakoryakov, S.Y. Misyura, S.L. Elistratov, R.A Dekhtyar, J. Eng. Thermophys. **23** (4), (2014)
4. V.E. Nakoryakov, S.Y. Misyura, S.L. Elistratov, JET **20(4)**, 1 (2011)
5. A.N. Pavlenko, V.V. Lel, Thermophysics and Aeromechanics **6(1)**, 105 (1999)
6. A.N. Pavlenko, A.S. Surtaev, Microgravity Sci. Tech. **22(2)**, 215 (2010)
7. K.V. Wong, O. De Leon, Adv. Mech. Eng. **2**, 519659 (2010)
8. S.J. Kim, I.C. Bang, J. Buongiorno, L.W. Hu. Bulletin of the Polish Academy of Sciences – Tech. Sciences **55**, 2 (2007)
9. H. Kim et al., ASME, ICNMM2009-82082 (2009)
10. L.D. Landau, JETP **14,** 6 (1944)
11. V.E. Zhukov, A.N. Pavlenko, M.I. Moiseev and D.V. Kuznetsov, Proc. of the 15th Int. Heat Transfer Conf. IHTC15-8766 (2014)